

Influence of the stray field of magnetic dot on the nucleation of superconductivity in a disk

D. S. Golubović*, W. V. Pogosov, M. Morelle and V. V. Moshchalkov
*Nanoscale Superconductivity and Magnetism Group,
 Laboratory for Solid State Physics and Magnetism ,
 K. U. Leuven, Celestijnenlaan 200 D, B-3001 Leuven, Belgium*

We have investigated the nucleation of superconductivity in an Al mesoscopic disk, with a magnetic dot on the top. The dot is magnetized perpendicularly, and its magnetic field is inhomogeneous. The Al disk and magnetic dot are separated by an insulating layer, which ensures that there is only magnetic interaction between them. This hybrid superconductor/ferromagnet structure exhibits the maximum critical temperature for a finite value of the perpendicular applied magnetic field, which is parallel to the magnetization of magnetic dot. We have found a good agreement between the experimental data for the superconductor/normal metal phase boundary and the theoretical predictions based on the Ginzburg-Landau theory.

PACS numbers: 74.78.Na, 74.25.Dw

I. INTRODUCTION

Hybrid superconductor/ferromagnet structures have attracted a lot of attention [1, 3, 4, 5, 6, 7, 8, 9, 10]. So far, the experimental efforts have mainly been focused on superconducting thin films with arrays of magnetic dots. Recently, a superconducting disk with a perpendicularly magnetized dot was fabricated and its superconducting $T_c(B)$ phase boundary determined [3]. However, the nucleation of superconductivity in this case was strongly affected by the proximity effect between the disk and dot.

In this paper we have investigated the onset of superconductivity in an Al disk with a perpendicularly magnetized Co/Pd magnetic dot on the top. The dot is separated from the disk by an insulating spacer layer, which ensures that there is no suppression of the order parameter in the disk due to the proximity effect and that the interaction between the disk and dot has only *magnetic* character [3].

The superconducting $T_c(B)$ phase boundary, obtained by transport measurements, exhibits an asymmetry with respect to the polarity of the applied magnetic field. The maximum critical temperature, higher than the zero-field critical temperature, is attained for a finite applied magnetic field which is parallel to the magnetization of magnetic dot.

II. SAMPLE PREPARATION AND EXPERIMENTAL TECHNIQUE

The sample was prepared on a SiO₂ substrate by electron beam lithography on PMMA950K and the co-polymer electron beam resists in three phases. Each phase involves the patterning of a desired structure, thermal evaporation of the material and ultrasonic assisted lift-off procedure.

The contact pads and leads, as well as the alignment markers are made up of 5 nm Cr and 30 nm Au. The superconducting disk is a 60 nm thick Al, whereas the magnetic dot consists of 2.5 nm Pd buffer layer and 10 bilayers of 0.4 nm Co and 1 nm Pd. A 10 nm thick Si spacer layer was evaporated before the magnetic dot. A careful alignment procedure was needed to position the dot at the centre of the disk.

Fig. 1 presents an atomic force microscopy image of the sample. The radius of the Al disk is 1.08 μm , whereas the dot has the radius of 270 nm. The electric contacts are wedge-shaped, with the opening angle of 15°, as these have proved to be the least invasive for transport measurements of superconducting nanostructures [14].

The magnetic properties of patterned Co/Pd structures were thoroughly investigated in Ref. [9]. We have determined the magnetic properties of the Co/Pd multilayer at room temperature from the magneto-optical Kerr measurements of the co-evaporated plane film. These data have confirmed that the Co/Pd multilayer has a perpendicular anisotropy, with a complete remanence and coercive field of approximately 70 mT. Prior to the measurements the sample was magnetized perpendicularly in the magnetic field of 300 mT. As the applied magnetic fields in the

* Dusan.Golubovic@fys.kuleuven.ac.be

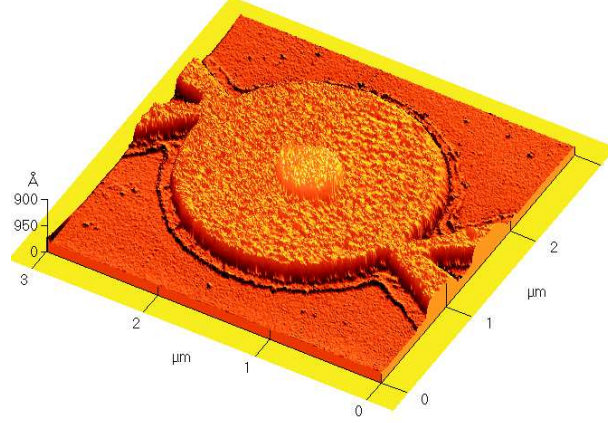


FIG. 1: An AFM topography image of the sample.

experiment never exceeded 30 mT, we have assumed that the magnetization of the dot remains unaltered during the measurements.

The onset of superconductivity in the structure was studied by measuring the superconducting $T_c(B)$ phase boundary. The phase boundary was found resistively, from four-point transport measurements, in a cryogenic setup at temperatures down to 1.11 K, with the temperature and field resolution of 0.5 mK and $5 \mu\text{T}$, respectively. The transport current with the effective value of 100 nA and frequency 27.7 Hz was used, whilst the signal-to-noise ratio was being improved by a lock-in amplifier.

The resistance of the structure at room temperature is 4.85Ω , the low temperature resistance is $R_n = 2.8 \Omega$, whereas the maximum critical temperature is $T_{cm} = 1.421 \text{ K}$.

III. EXPERIMENTAL RESULTS

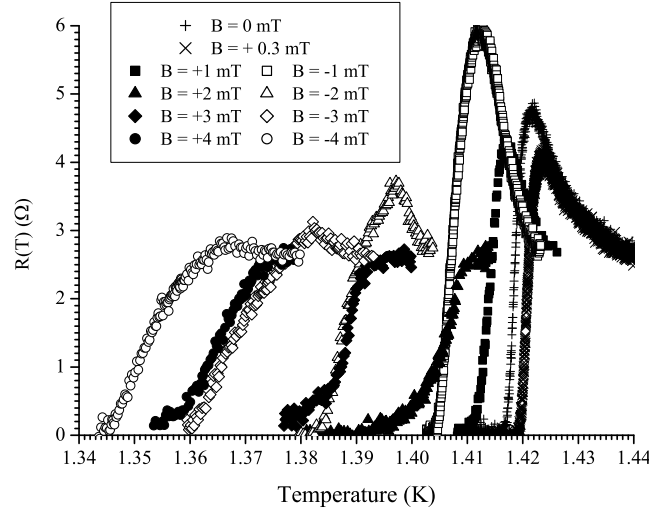


FIG. 2: $R(T)$ transition in different applied magnetic fields. Filled symbols indicate the transitions in the applied fields parallel to the magnetization of the dot, whereas open symbols present the transition in the antiparallel magnetic fields.

Fig. 2 presents resistive transitions of the structure in a constant applied magnetic field. We have taken parallel magnetic fields as positive and antiparallel magnetic fields as negative, and will be using this convention throughout the paper.

Typically, superconducting structures have resistive transitions that are symmetric with respect to the polarity of an applied magnetic field. Likewise, the maximum transition temperature is achieved in zero applied field. The transitions in Fig. 2 are strongly asymmetric with respect to the polarity of an applied field. The critical temperature, defined conventionally as the temperature at which the resistance is $R_n/2$, in the applied magnetic field of $+2$ mT is equal to the transition temperature in -1 mT. This dependence of the resistive transitions on the field polarity is reproduced for higher fields, as well. More importantly, the critical temperature in zero applied field is not the maximum critical temperature of the structure. The structure attains the maximum critical temperature when exposed to the magnetic field of $+0.3$ mT. The difference between the maximum and zero-field critical temperature is approximately 2.5 mK.

The transitions for the applied fields $-1 < B_a < 1$ [mT] have considerable overshoots in resistance, with respect to the normal state. This phenomenon is related to the formation of normal/superconducting (NS) interfaces and nonequilibrium charge imbalance effects [11, 13, 14]. The critical temperature of the mesoscopic contacts is slightly higher than the critical temperature of the disk [14]. For this reason, superconductivity nucleates nonuniformly, thus giving rise to the formation of the NS interfaces. Due to a finite local magnetic induction in the disk generated by the dot, the difference in the critical temperatures of the disk and the mesoscopic contacts is greater than for a disk without a magnetic dot. As a positive applied magnetic field increases, the total magnetic induction in the disk around the magnetic dot decreases, thereby effectively reducing the difference in the critical temperatures of the disk and mesoscopic contacts. For this reason, as the positive applied field increases the amplitude of the resistance anomaly decreases. On the other hand, a negative applied field gives rise to a greater difference in the local critical temperatures, which is responsible for more pronounced peaks. When increasing the negative applied field, the contribution of the stray field to the total field becomes less significant and the typical amplitudes of the overshoots are recovered [1, 14].

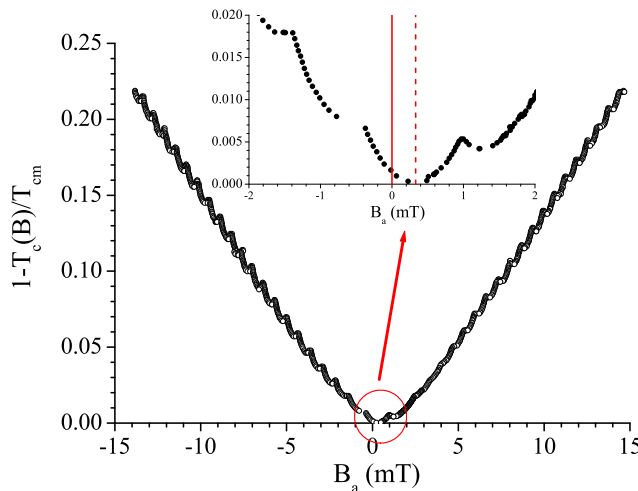


FIG. 3: The experimentally obtained superconducting phase boundary plotted as $1 - T_c(B)/T_{cm}$ versus the applied field B_a . T_{cm} is the maximum critical temperature. The inset shows the phase boundary around T_{c0} .

Fig. 3 shows the experimental phase boundary in the plane of the normalized critical temperature $1 - T_c(B)/T_{cm}$ and the applied magnetic field, with T_{cm} being the maximum measured critical temperature. The inset displays the phase boundary around the zero-field critical temperature T_{c0} . The phase boundary, except for the low fields, has a *linear* background, which is the hallmark of the nucleation process in the disk [1]. In addition, the quasiperiodicity of the phase boundary is entirely consistent with what has been obtained for a mesoscopic superconducting disk without the dot [2]. When there is a pronounced proximity effect between the superconducting disk and magnetic dot, the order parameter is suppressed below the dot and the disk can be approximated with a superconducting loop with a finite width [3]. In this case, the superconducting $T_c(B)$ phase boundary has a crossover in the background - from a parabolic for low fields to a linear for high fields [2]. Therefore, the presence of a pronounced proximity effect between the dot and the disk can confidently be ruled out, and specific features of the phase boundary can be attributed to the magnetic interaction between the disk and magnetic dot.

The most striking feature of the phase boundary is its asymmetry. The minimum in the phase boundary, which corresponds to the maximum critical temperature of the structure, has been obtained for a finite applied magnetic field which is parallel to the magnetization of magnetic dot.

IV. THEORETICAL RESULTS

The experimental data have been analysed by using the Ginzburg-Landau (GL) theory. Near the transition from the normal to the superconducting state the total magnetic field in the disk is equal to the sum of the stray field of the magnetic dot and a uniform externally applied field. The stray field we have used in the analysis, was obtained by magnetostatic calculations. For details, we refer to [3, 6].

As the sample in our experiment is thinner than the coherence length $\xi(T)$, the order parameter is constant along z axis and the magnetic field in the GL equations can be averaged out over the thickness of the disk. Thus, the problem is reduced to the 2D case. The axial symmetry of the sample allows us to further reduce the dimensionality of the problem to the 1D case, since near the phase boundary the modulus of the order parameter is axially symmetric. Using the cylindrical coordinate system with coordinates r, φ, z , the dimensionless order parameter $\psi(r, \phi)$ can be expressed as

$$\psi(r, \phi) = f(r) \exp(-iL\phi), \quad (1)$$

where $f(r)$ is the modulus of the order parameter and L stands for the winding number (vorticity). Instead of solving the GL equations, which are nonlinear with respect to $f(r)$, we have applied a variational procedure, similar to what has been used in Ref. [12]. The trial function used for the modulus of the order parameter is

$$f(r) = p_1 \cdot \exp\left(-q \frac{r^2}{R^2}\right) \cdot \left(\left(\frac{r}{R}\right)^L + p_2 \left(\frac{r}{R}\right)^{L+1} + p_3 \left(\frac{r}{R}\right)^{L+2} + p_4 \left(\frac{r}{R}\right)^{L+3}\right). \quad (2)$$

where p_1, p_2, p_3 and p_4 are the variational parameters, R is the radius of the disk, whereas q is found from the vacuum boundary condition for the order parameter ($f'(R) = 0$)

$$q = \frac{L + p_2(L+1) + p_3(L+2) + p_4(L+3)}{2(1 + p_2 + p_3 + p_4)}. \quad (3)$$

Using Eqs. (1) and (2) the GL energy is found as a function of the variational parameters (see Ref. [12]). The values of the variational parameters are calculated by minimizing the GL energy. Comparing the energies of states with different L the superconducting $T_c(B)$ phase boundary of the disk is found.

Fig. 4 displays the theoretical fit of the experimental phase boundary in the low field regime, along with the theoretical phase boundary of an identical superconducting disk without magnetic dot (dashed line). The critical temperatures are normalized to the zero-field critical temperature of the superconducting disk without magnetic dot, as obtained by the calculations. The best agreement between the theory and the experiment has been found for $\xi(T = 0) = 90$ nm, which is consistent with the value of $\xi(T = 0)$ obtained in Ref. [1] for mesoscopic Al superconductors. Each cusp in the phase boundary corresponds to the transition between the states with different vorticities. According to our results, there is one vortex in the disk in the absence of the external magnetic field.

The superconducting phase boundary strongly depends upon the polarity of an external magnetic field. The magnetization of the dot m has been chosen to provide the best qualitative and quantitative agreement between the theory and the experiment in the vicinity of T_{c0} . The direction of the shift of $T_c(B)$ phase boundary near T_{c0} , for a fixed orientation of the magnetization m , depends upon the intensity of the stray field of magnetic dot. The shift can come about as a result of the cancellation of the total flux generated by the magnetic dot, or due to a change in the kinetic energy of the superconducting condensate in the disk, accompanied by a switch in the vorticity by one. The former shifts the phase boundary in the direction opposite to the magnetization of the dot and the maximum critical temperature is observed for a finite *negative* applied field, whereas the latter provides that the maximum critical temperature is achieved for a finite applied field parallel to the magnetization of the dot, that is for a finite *positive* field. Which of these competing effects prevails strongly depends upon the intensity of magnetization of magnetic dot, as well as upon the parameters of the superconducting structure. In our case the shift is positive.

In addition to the shift along the B -axis, the phase boundary of the hybrid structure is also shifted along the T -axis. The shift along the T -axis is caused by a difference in the maximum critical temperature of the disk with and without the dot. As the stray field of the dot is spatially inhomogeneous, it cannot be cancelled out by an externally applied homogeneous magnetic field. For this reason, there is always a finite flux through a disk with a magnetic dot and its maximum critical temperature is reduced compared to the disk without a magnetic dot. Even though the maximum critical temperature of the hybrid structure is less than 1% lower than the maximum critical temperature of the plane disk, this difference is sufficient to modify the phase boundary. If the additional homogeneous magnetic field were applied, there would be no differences in maximum critical temperature, and, consequently, the $T_c(B)$ phase boundary would not be substantially modified along the T -axis. We can, therefore, conclude that the effect of the *inhomogeneous* magnetic field on the nucleation of superconductivity is *twofold*: it shifts the phase boundary along

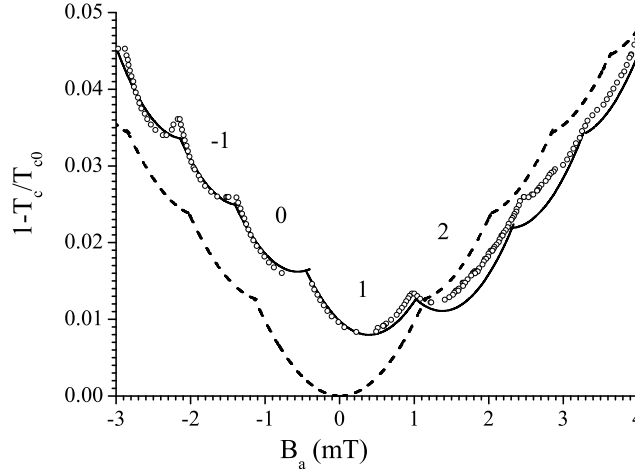


FIG. 4: The experimental data and the corresponding theoretical phase boundary of the superconducting disk with magnetic dot (solid line), as well as the theoretical phase boundary of an identical superconducting disk without magnetic dot (dashed line). The temperatures are normalized to the zero-field critical temperature of the disk without magnetic dot. The numbers indicate the vorticity of the hybrid structure.

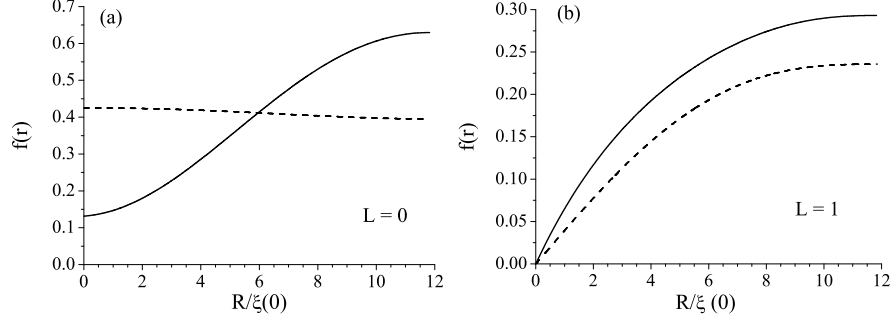


FIG. 5: The moduli of the order parameter in (a) the Meissner state and (b) vortex state with the vorticity $L = 1$. The solid line describes the superconducting disk with magnetic dot, whereas the dashed line presents the disk without magnetic dot. In the Meissner state the temperatures are $T/T_{c0} = 0.987$ and $T/T_{c0} = 0.995$ for the disk with and without magnetic dot, respectively. For the vortex state $L = 1$ the respective temperatures are $T/T_{c0} = 0.990$ and $T/T_{c0} = 0.995$. Here T_{c0} is the zero-field temperature of the plane superconducting disk.

the B -axis, as well as distorts the phase boundary along the T -axis, altering the values at which the structure switches between different vorticities.

The stray field of the magnetic may change the typical spatial profile of the superconducting condensate density within the disk. Fig. 5(a) and 5(b) present the moduli of the order parameter for the disk with magnetic dot (solid line) and disk without magnetic dot (dashed line). Fig. 5(a) shows the Meissner state, whereas Fig. 5(b) shows the state with the vorticity $L = 1$. In the Meissner state, for the plane superconducting disk, the modulus of the order parameter has a maximum at the centre of the disk. On the other hand, the amplitude of the order parameter is reduced below the magnetic dot, where the intensity of the stray field is the highest, and exhibits a minimum at the centre of the disk. The spatial profile of the order parameter is not strongly affected by the stray field in the vortex state, because the vortex core, where the order parameter is equal to zero, is in the region below the dot.

In conclusion, we have fabricated a mesoscopic superconducting disk made up of Al with a perpendicularly magnetized magnetic dot on the top. The superconducting properties of the system have been investigated by measuring the superconducting/normal state phase boundary $T_c(B)$. It has been demonstrated that the phase boundary is asymmetric with respect to the direction of the applied field. The maximum critical temperature has been attained for a finite value of the applied magnetic field, which is oriented parallel to the magnetization of magnetic dot. The experimental data are in a good agreement with the theoretical results. It has also been shown that the inhomogeneity of the stray field gives rise to a modification of the $T_c(B)$ phase boundary along the T -axis, which would not be present if an additional magnetic field were homogeneous.

V. ACKNOWLEDGEMENTS

The authors would like to thank G. Rens for AFM measurements. This work has been supported by the Belgian IUAP, the Flemish FWO and the Research Fund K. U. Leuven GOA/2004/02 programmes, as well as by the ESF programme "VORTEX". W. V. P. acknowledges the support from the Research Council of the K.U. Leuven and DWTC.

-
- [1] MOSHCHALKOV V. V. *et al.*, in Handbook of Nanostructured Materials and Nanotechnology 3, edited by H. S. Nalwa (Academic Press, San Diego) 2000, pp. 451-525.
 - [2] BRUYNDONCX V. *et al.*, Phys. Rev. B, **60**, 10468 (1999).
 - [3] GOLUBOVIĆ D. S. *et al.*, Appl. Phys. Lett., **83**, 1593 (2003).
 - [4] POKROVSKY V. L. *et al.*, cond-mat/0305153 (2003).
 - [5] ALADYSHKIN A. Yu. *et al.*, cond-mat/0305551 (2003).
 - [6] MILOŠEVIĆ M. V. *et al.*, Phys. Rev. B, **66**, 024515 (2002).
 - [7] MILOŠEVIĆ M. V. *et al.*, Phys. Rev. B, **66**, 174519 (2002).
 - [8] VAN BAEL M. J. *et al.*, Phys. Rev. Lett., **86**, 1 (2001).
 - [9] LANGE M. *et al.*, Phys. Rev. Lett., **90**, 197006 (2003).
 - [10] VAN BAEL M. J. *et al.*, Physica C, **332**, 12 (2000).
 - [11] STRUNK C. *et al.*, Phys. Rev. B, **54**, R12701 (1996).
 - [12] POGOSOV W.V., Phys. Rev. B, **65**, 224511 (2002).
 - [13] BRUYNDONCX V. *et al.*, Europhys. Lett. **60**, 6 (1996).
 - [14] MORELLE M. *et al.*, Phys. Stat. Sol., **237**, 1 (2003).